Published May 1, 1999

Four Kinetically Distinct Depolarization-activated K^+ Currents in Adult Mouse Ventricular Myocytes

Haodong Xu, Weinong Guo, and Jeanne M. Nerbonne

From the Department of Molecular Biology and Pharmacology, Washington University School of Medicine, St. Louis, Missouri 63110

ABSTRACT In the experiments here, the time- and voltage-dependent properties of the Ca^{2+}-independent, depolarization-activated K^+ currents in adult mouse ventricular myocytes were characterized in detail. In the majority (65 of 72, ≈90%) of cells dispersed from the ventricles, analysis of the decay phases of the outward currents revealed three distinct K^+ current components: a rapidly inactivating, transient outward K^+ current, $I_{to,f}$ (mean ± SEM τ_{decay} = 85 ± 2 ms); a slowly (mean ± SEM τ_{decay} = 1,162 ± 29 ms) inactivating K^+ current, $I_{K,slow}$; and a non inactivating, steady state current, I_{ss}. In a small subset (7 of 72, ≈10%) of cells, $I_{to,f}$ was absent and a slowly inactivating (mean ± SEM τ_{decay} = 196 ± 7 ms) transient outward current, referred to as $I_{to,s}$, was identified; the densities and properties of $I_{K,slow}$ and I_{ss} in $I_{to,s}$-expressing cells are indistinguishable from the corresponding currents in cells with $I_{to,f}$. Microdissection techniques were used to remove tissue pieces from the left ventricular apex and from the ventricular septum to allow the hypothesis that there are regional differences in $I_{to,f}$ and $I_{to,s}$ expression to be tested directly. Electrophysiological recordings revealed that all cells isolated from the apex express $I_{to,f}$ (n = 35); $I_{to,s}$ is not detected in these cells (n = 35). In the septum, by contrast, all of the cells express $I_{to,s}$ (n = 28) and in the majority (22 of 28, 80%) of cells, $I_{to,f}$ is also present. The density of $I_{to,f}$ (mean ± SEM at +40 mV = 6.8 ± 0.5 pA/pF, n = 22) in septum cells, however, is significantly ($P < 0.001$) lower than $I_{to,f}$ density in cells from the apex (mean ± SEM at +40 mV = 34.6 ± 2.6 pA/pF, n = 35). In addition to differences in inactivation kinetics, $I_{to,f}$, $I_{to,s}$, and $I_{K,slow}$ display distinct rates of recovery (from inactivation), as well as differential sensitivities to 4-aminopyridine (4-AP), tetraethylammonium (TEA), and *Heteropoda* toxin-3. $I_{K,slow}$, for example, is blocked selectively by low (10–50 μM) concentrations of 4-AP and by (≥25 mM) TEA. Although both $I_{to,f}$ and $I_{to,s}$ are blocked by high (>100 μM) 4-AP concentrations and are relatively insensitive to TEA, $I_{to,f}$ is selectively blocked by nanomolar concentrations of *Heteropoda* toxin-3, and $I_{to,s}$ (as well as $I_{K,slow}$ and I_{ss}) is unaffected. I_{ss} is partially blocked by high concentrations of 4-AP or TEA. The functional implications of the distinct properties and expression patterns of $I_{to,f}$ and $I_{to,s}$, as well as the likely molecular correlates of these (and the $I_{K,slow}$ and I_{ss}) currents, are discussed.

KEY WORDS: $I_{to,f}$ • $I_{to,s}$ • transient outward currents • delayed rectifier • transgenic mice

introduction

Depolarization-activated K^+ currents play key roles in determining the amplitudes and durations of action potentials in cardiac cells, and several distinct types of voltage-gated K^+ channels that subserve these functions have been identified (for reviews, see Anumonwo et al., 1991; Campbell et al., 1995; Kass, 1995; Barry and Nerbonne, 1996; Giles et al., 1996). This diversity has a physiological significance in the heart in that the various K^+ currents underlie distinct phases of action potential repolarization (Anumonwo et al., 1991; Campbell et al., 1995; Kass, 1995; Barry and Nerbonne, 1996; Giles et al., 1996), and cell type–specific differences in K^+ channel expression contribute to regional variations in action potential waveforms (Antzelevitch et al., 1995; Barry and Nerbonne, 1996). Voltage-gated K^+ channels are primary targets for the actions of a variety of endogenous neurotransmitters and neurohormones, as well as exogenous drugs that modulate cardiac functioning (Anumonwo et al., 1991; Gadsby, 1995). In addition, changes in the densities and/or the properties of K^+ currents occur in conjunction with myocardial damage or disease and these changes can have profound physiological consequences, including leading to the generation of life threatening arrhythmias (Ten Eick et al., 1989; Näbauer et al., 1993; Boyden and Jeck, 1995; Wilde and Veldkamp, 1997; VanWagoner et al., 1997; Näbauer and Kääb, 1998). For all of these reasons, there is considerable interest in defining the molecular correlates of functional cardiac K^+ channels (Barry and Nerbonne, 1996; Deal et al., 1996), and in understanding the mechanisms controlling the

Address correspondence to Dr. Jeanne M. Nerbonne, Department of Molecular Biology and Pharmacology, Washington University School of Medicine, 660 South Euclid Avenue, Box 8103, St. Louis, MO 63110. Fax: 314-362-7058; E-mail: jnerbonn@pharmdec.wustl.edu

Published May 1, 1999

regulation, modulation, and functional expression of these channels.

A number of voltage-gated K^+ channel pore-forming (α) and accessory (β) subunits have now been cloned from heart cDNA libraries, and a variety of experimental approaches are being exploited to probe the molecular basis of functional K^+ channel diversity in mammalian cardiac cells (for reviews, see Barry and Nerbonne, 1996; Deal et al., 1996; Nerbonne, 1998). Of these, transgenic and knockout strategies seem particularly promising because the functional consequences of manipulating K^+ channel expression in vivo can also be explored directly. Indeed, mice with targeted Kv α subunit deletions, including Kv3.1, Kv1.1, and Kv1.4, have been described recently (Ho et al., 1997; London et al., 1998b; Smart et al., 1998). None of these animals appears to display a cardiac phenotype, however, leading to suggestions that Kv1.1, Kv3.1, and Kv1.4 likely do not play roles in the generation of functional cardiac K^+ channels, at least in the mouse (Ho et al., 1997; London et al., 1998b; Smart et al., 1998). London et al. (1998a), however, recently reported the generation of transgenic mice expressing a truncated Kv1.1 (*Kv1.1N206Tag*), driven by the α-myosin heavy chain promoter to direct cardiac-specific expression of the transgene (Lyons et al., 1990; Ng et al., 1991; Palermo et al., 1996). In vitro, *Kv1.1N206Tag* functions as a dominant negative, reducing or eliminating heterologously expressed Kv1.4 and Kv1.5 currents (Folco et al., 1997). In ventricular myocytes isolated from *Kv1.1N206Tag*-expressing mice, a 4-aminopyridine–sensitive, slowly decaying outward K^+ current, $I_{K,slow}$, was found to be selectively attenuated (London et al., 1998a). In addition, action potentials and QT intervals are prolonged in the *Kv1.1N206Tag*-expressing transgenics, and electrocardiographic recordings revealed increased frequency of premature ventricular beats and spontaneous ventricular tachycardia in these animals (London et al., 1998a).

A dominant negative strategy has also been exploited by Barry et al. (1998) in studies focussed on identifying the molecular correlate of the cardiac transient outward K^+ current, I_{to}. Using an approach previously used to make Kv1 α subunits that gate on membrane depolarization but do not conduct (Perozo et al., 1993; Ribera, 1996), mutations were introduced into the coding sequence of the pore region of Kv4.2 to convert the tryptophan (W) in position 362 to phenylalanine (F) to produce Kv4.2W362F, and, in in vitro experiments, Kv4.2W362F was shown to function as a dominant negative against Kv4.2 and Kv4.3 (Barry et al., 1998). In ventricular myocytes isolated from Kv4.2W362F-expressing animals, I_{to} ($I_{to,f}$) is eliminated, and action potential durations are increased significantly (Barry et al., 1998). Although QT intervals are also markedly prolonged in Kv4.2W362F-expressing transgenics, these animals do not develop spontaneous arrhythmias (Barry et al., 1998). However, a "novel" rapidly activating, slowly inactivating K^+ current, not clearly evident in wild-type cells, was identified in ventricular myocytes isolated from Kv4.2W362F-expressing animals, an observation interpreted as suggesting that electrical remodeling occurs in the myocardium when the expression of endogenous K^+ channels is altered (Barry et al., 1998).

In spite of the growing interest in using transgenic and knockout mice, the electrophysiological properties of adult mouse cardiac myocytes have not been characterized in detail to date. This fact and the finding of the novel K^+ current in Kv4.2W362F-expressing ventricular myocytes prompted us to undertake studies focussed on examining the time- and voltage-dependent properties and the pharmacological sensitivities of the voltage-gated K^+ currents in adult mouse ventricular myocytes. The results of these experiments reveal the presence of four kinetically and pharmacologically distinct voltage-gated K^+ currents in these cells: (a) a rapidly activating and inactivating, "fast transient" K^+ current, $I_{to,f}$; (b) a rapidly activating, slowly inactivating, "slow transient" current, $I_{to,s}$; (c) a rapidly activating, very slowly inactivating current, $I_{K,slow}$; and (d) a slowly activating, noninactivating K^+ current, I_{ss}. Interestingly, the results presented here reveal that $I_{K,slow}$ and I_{ss} are expressed in all adult mouse ventricular cells, whereas $I_{to,f}$ and $I_{to,s}$ are differentially distributed.

materials and methods

Preparation of Isolated Myocytes

Ventricular myocytes were isolated from adult (after postnatal day 45) C57BL6 mice using a procedure previously developed and used to isolate rat cardiomyocytes (Xu et al., 1996). In brief, hearts were excised from anesthetized (5% halothane/95% O_2) adult animals, mounted on a Langendorf apparatus, and perfused retrogradely through the aorta with 40 ml of a Ca^{2+}-free HEPES-buffered Earles balanced salt solution (Gibco Laboratories) supplemented with 6 mM glucose, amino acids, and vitamins (Buffer A). Hearts were then perfused with 50 ml of Buffer A containing 0.8 mg/ml collagenase B (Boehringer Mannheim Biochemicals) and 10 μM $CaCl_2$, and the temperature of the tissue and the perfusate were maintained at 34–35°C. The enzyme solution was filtered (at 5 μm) and recirculated through the heart for ~15–20 min.

In initial experiments, the lower two thirds of the left and right ventricles were removed after the perfusion, and, after mincing in enzyme-containing Buffer A, were transferred to fresh (enzyme-free) Buffer A supplemented with 1.25 mg/ml taurine, 5 mg/ml bovine serum albumin (Sigma Chemical Co.), and 150 μM $CaCl_2$ (Buffer B). In experiments focussed on determining whether there are regional differences in K^+ current expression, the heart was cut open after perfusion, and the ventricular septum and the top ~0.3 mm of tissue at the apex of the left ventricle were removed. The tissue pieces from the apex and septum were placed separately in fresh Buffer B. After mechanical dispersion (by gentle trituration), cell suspensions were filtered to remove large undissociated tissue fragments, and cells were collected by

Published May 1, 1999

sedimentation. Isolated myocytes were resuspended in fresh Buffer B, plated on laminin-coated coverslips, and placed in a 95% air/5% CO_2 incubator at 37°C. Approximately 30 min after plating, serum-free medium-199 (M-199; Irvine Scientific), supplemented with antibiotics (penicillin/streptomycin), was added. Ca^{2+}-tolerant ventricular myocytes adhered to the laminin, and damaged cells were removed by replacing the medium with fresh M-199 ≈1 h after plating. Cells were examined electrophysiologically within 48 h of isolation.

Electrophysiological Recordings

The conventional whole-cell gigaohm seal recording technique (Hamill et al., 1981) was employed to record Ca^{2+}-independent, depolarization-activated K^+ currents from isolated adult mouse ventricular myocytes. Electrophysiological recordings were only obtained from Ca^{2+}-tolerant, rod-shaped ventricular cells, and all experiments were conducted at room temperature (22–24°C). The bath solution contained (mM): 136 NaCl, 4 KCl, 1 $CaCl_2$, 2 $MgCl_2$, 5 $CoCl_2$, 10 HEPES, 0.02 tetrodotoxin, and 10 glucose, pH 7.35, and 295–305 mOsm. Recording pipettes contained (mM): 135 KCl, 1 $MgCl_2$, 10 EGTA, 10 HEPES, 5 glucose, pH 7.2, and 300–310 mOsm. α-dendrotoxin (α-DTX; Alamone Labs),[1] *Heteropoda* toxin-3 (HpTx-3; NPS Pharmaceuticals), and 4-aminopyridine (4-AP; Sigma Chemical Co.) stock solutions were prepared in distilled water, and diluted to the appropriate concentration in bath solution immediately before use. Tetraethylammonium (TEA; Sigma Chemical Co.)-containing bath solutions were prepared by equimolar substitution of TEACl for NaCl in the standard bath solution. α-DTX, HpTx-3, 4-AP, or TEA was applied to isolated myocytes during recordings using narrow-bore capillary tubes (300 μm i.d.) placed within ≈200 μm of the cell.

Experiments were conducted using an Axopatch-1D (β = 1) (Axon Instruments) or a Dagan 3900A (Dagan Corp.) amplifier. Recording pipettes, fabricated from soda lime glass, had tip diameters of 1–2 μm and resistances of 2–3 MΩ when filled with recording solution. Tip potentials were zeroed before membrane pipette seals were formed; seal resistances were ≥5 GΩ. After establishing the whole-cell configuration, ±10-mV steps were applied to allow measurement of whole cell membrane capacitances and input resistances. Series resistances were estimated by dividing the time constant of the decay of the capacitative transient by the membrane capacitance. Whole-cell membrane capacitances and series resistance were routinely compensated (≥85%) electronically; voltage errors resulting from the uncompensated series resistance were ≤8 mV and were not corrected. Only data obtained from cells with input resistance ≥0.7 GΩ were analyzed. Voltage-gated outward K^+ currents were routinely evoked during 500-ms or 4.5-s depolarizing voltage steps to potentials between −40 and +60 mV from a holding potential of −70 mV; voltage steps were presented in 10-mV increments at 15-s intervals. Experiments were controlled and data were collected using a Gateway 300 MHz microcomputer equipped with a Digidata 1200 (Axon Instruments) analogue/digital interface and pClamp 6.1 (Axon Instruments). Data were acquired at variable sampling frequencies (ranging from 0.1 to 50 kHz), and current signals were filtered on-line at 5 kHz before digitization and storage.

Data Analysis

Analyses of digitized data were completed using pClamp 6.1. Whole-cell membrane capacitances were determined by integrating the capacitative transients evoked during ±10-mV voltage steps from a holding potential of −70 mV (before series resistance and capacity compensation). Peak currents at each test potential were measured as the difference between the maximal outward current amplitudes and the zero current level. The waveforms of the 4-AP–, TEA-, and α-DTX–sensitive currents were determined by subtraction of the currents recorded in the presence of 4-AP, TEA, or α-DTX from the control currents (in the same cell).

Activation time constants were determined from single exponential fits to the rising phases of the outward K^+ currents evoked during depolarizing voltage steps to test potentials between 0 and +60 mV from a holding potential of −70 mV; the fits were constrained to data points acquired 300 μs after the onset of the voltage step (thereby ignoring the delay) to the peak of the outward current. The decay phases of the currents evoked during long (4.5 s) depolarizing voltage steps to test potentials between +10 and +60 mV from a holding potential of −70 mV were fitted by the sum of two or three exponentials using one of the following expressions: $y(t) = A_1 * \exp(-t/\tau_1) + A_2 * \exp(-t/\tau_2) + A_{ss}$ or $y(t) = A_1 * \exp(-t/\tau_1) + A_2 * \exp(-t/\tau_2) + A_3 * \exp(-t/\tau_3) + A_{ss}$, where t is time, τ_1, τ_2, and τ_3 are the time constants of decay of the inactivating K^+ currents, A_1, A_2, and A_3 are the amplitudes of the inactivating current components, and A_{ss} is the amplitude of the steady state, noninactivating component of the total outward K^+ current. For all fits, time zero was set at the peak of the outward current. For all analyses, correlation coefficients (R) were determined to assess the quality of fits, R values for the fits reported here were ≥0.98. All averaged and normalized data are presented as means ± SEM. The statistical significance of observed differences between groups of cells or between different parameters describing the properties of the currents were evaluated using a one way analysis of variance or a two-tailed Student's t test; P values are presented in the text, and statistical significance was set at $P < 0.05$.

results

Depolarization-activated Currents in Adult Mouse Ventricular Myocytes

In the initial experiments here, whole-cell depolarization-activated outward K^+ currents in myocytes isolated from the (lower two thirds of the left and right) ventricles of adult C57BL6 mice were recorded and analyzed (see MATERIALS AND METHODS). With voltage-gated Ca^{2+} and Na^+ currents blocked, outward currents were routinely recorded during 500-ms (Fig. 1, A and C) and 4.5-s (Fig. 1, B and D) depolarizing voltage steps to potentials between −40 and +60 mV from a −70-mV holding potential (n = 72). The rates of rise and the amplitudes of the currents increase with increasing depolarization; the largest and most rapidly activating current in Fig. 1 was evoked at +60 mV. No outward K^+ currents were recorded during depolarizing voltage steps when the K^+ in the pipettes was replaced by Cs^+ (n = 6). The currents characterized here, therefore, reflect only the activation of Ca^{2+}-independent, depolarization-activated K^+ channels.

Although the outward K^+ currents in all cells activated rapidly, the absolute current amplitudes (densities) and the decay phases of the currents were some-

[1]*Abbreviations used in this paper:* 4-AP, 4-aminopyridine; DTX, dendrotoxin; HpTx-3, *Heteropoda* toxin 3; TEA, tetraethylammonium.

Published May 1, 1999

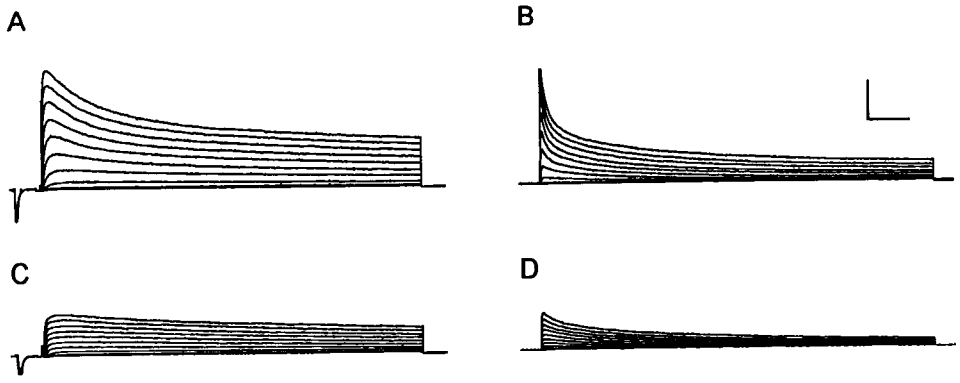

FIGURE 1. Differences in the waveforms of the Ca^{2+}-independent, depolarization-activated K^+ currents in myocytes randomly dispersed from adult mouse (left and right) ventricles. Whole-cell outward K^+ currents were evoked during 500-ms (A and C) and 4.5-s (B and D) depolarizing voltage steps to potentials between −40 and +60 mV from a holding potential of −70 mV; each trial was preceded by a brief (20 ms) depolarization to −20 mV to eliminate contamination from voltage-gated inward Na^+ currents not blocked completely by tetrodotoxin (note the inward currents at early times in the records in A and C). The records in A and B were obtained from the same cell, and those in C and D were from the same cell; only the durations of the voltage steps in A and B (and C and D) are different. As is evident, peak outward current amplitudes in A and B are substantially larger than those in C and D. In addition, the decay phases of the outward K^+ currents in C and D are slower than those in A and B; the rapidly inactivating transient outward K^+ current, $I_{to,f}$, is not evident in the records in C and D (see text). Scale bars: A and B, 4 nA and 55 ms; B and D, 4 nA and 500 ms.

what variable among cells (Fig. 1). In the majority of cells (65 of 72, ≈90%), outward current waveforms similar to those in Fig. 1, A and B, were recorded. There is a rapid component of current decay in these cells, consistent with the presence of a transient outward K^+ current, previously described in these cells (Benndorf and Nilius, 1988; Wang and Duff, 1997), as well as in cardiac myocytes in other species (Campbell et al., 1995; Barry and Nerbonne, 1996; Giles et al., 1996). We refer to this current as $I_{to,\,fast}$, or $I_{to,f}$, to distinguish it from another, more slowly inactivating, transient outward K^+ current, $I_{to,slow}$, or $I_{to,s}$, seen in some cells (see below). As noted in the INTRODUCTION, it was recently demonstrated that $I_{to,f}$ is eliminated in adult mouse ventricular myocytes isolated from animals expressing a mutant Kv4.2 α subunit (Kv4.2W362F) that functions as a dominant negative (Barry et al., 1998), an observation consistent with previous suggestions that members of the Kv4 α subunit subfamily underlie cardiac $I_{to,f}$ (Dixon and McKinnon, 1994; Barry et al., 1995; Dixon et al., 1996).

In the other (7 of 72, ≈10%) cells studied in these initial experiments, $I_{to,f}$ was not evident (Fig. 1, C and D). Peak outward K^+ current densities in this subset of cells were significantly ($P < 0.001$) lower than in the cells with $I_{to,f}$; the mean ± SEM peak outward K^+ current densities at +40 mV in cells with and without $I_{to,f}$, for example, were 47.0 ± 2.5 ($n = 65$) and 31.5 ± 4.1 ($n = 7$) pA/pF, respectively (Table I). In other respects, however, the properties of the cells with and without $I_{to,f}$ were indistinguishable; for example, the mean ± SEM whole cell membrane capacitances and input resistances were 142 ± 4 pF and 1.00 ± 0.09 GΩ for the cells with $I_{to,f}$ ($n = 65$) and 151 ± 14 pF and 0.95 ± 0.15 GΩ for the cells lacking $I_{to,f}$ ($n = 7$). Subsequent experiments were focussed, therefore, on characterizing the depolarization-activated K^+ current components in these cells in further detail.

Multiple K^+ Current Components in Adult Mouse Ventricular Myocytes

Analysis of the decay phases of the outward K^+ currents evoked during long depolarizations in the majority of cells (Fig. 1 B) revealed that current decay is well described by the sum of two exponentials, with decay time constants (τ_{decay}) that differ by an order of magnitude, and a noninactivating (i.e., steady state) current. The mean ± SEM τ_{decay} ($n = 65$) for the fast and slow components derived from these fits were 85 ± 2 and 1,162 ± 29 ms (Table I); neither time constant displays any ap-

TABLE I

Four Distinct Outward K^+ Currents in Mouse Ventricular Myocytes

Cells	I_{peak}	$I_{to,f}$	$I_{to,s}$	$I_{K,slow}$	I_{ss}
With I_{to}					
τ_{decay} (ms)	—	85 ± 2	—	1162 ± 29	—
Density*					
(pA/pF)	47.0 ± 2.5	26.2 ± 1.6	—	14.9 ± 0.9	5.5 ± 0.3
Percent I_{peak}	—	56	—	32	12
n	65	65	—	65	65
Without $I_{to,f}$					
τ_{decay} (ms)	—	—	196 ± 7	1368 ± 101	NA
Density*					
(pA/pF)	31.5 ± 4.1	—	11.4 ± 1.9	15.6 ± 2.1	4.5 ± 0.5
Percent I_{peak}	—	—	36	50	14
n	7	—	7	7	7

*Current densities were determined from analyses of records obtained on depolarization to +40 mV from a holding potential of −70 mV; all values are means ± SEM.

Published May 1, 1999

preciable voltage dependence (Fig. 2 A). Two components of outward K^+ current decay (with τ_{decay} values of 80 ms and 1 s) in adult mouse ventricular myocytes were previously described, although both were attributed to inactivation of I_{to} (Wang and Duff, 1997). In another recent study, however, the two components of inactivation were considered distinct current components: the rapidly inactivating current was referred to as I_{to} and the slowly inactivating current was termed $I_{K,slow}$ (London et al., 1998a; Zhou et al., 1998). Consistent with this distinction, $I_{K,slow}$ was selectively attenuated in ventricular myocytes isolated from transgenic mice expressing a truncated Kv1.1 construct, *Kv1.1N206Tag* (London et al., 1998a) that functions as a dominant negative (Folco et al., 1997). These observations were interpreted as suggesting that Kv1 α subunits, likely Kv1.5, underlie mouse ventricular $I_{K,slow}$ (London et al., 1998a). The slowly decaying current component will also be referred to here as $I_{K,slow}$ and as noted above the rapidly inactivating current is referred to as $I_{to,f}$ to distinguish it from $I_{to,s}$.

The densities of $I_{to,f}$ and $I_{K,slow}$ vary considerably among cells. For $I_{to,f}$, for example, the peak current density at +40 mV ranged from 7.9 to 62.4 pA/pF, with a mean ± SEM of 26.2 ± 1.6 pA/pF (n = 65; Table I). $I_{K,slow}$ density at +40 mV ranged from 2.8 to 39.9 pA/pF with a mean ± SEM of 14.9 ± 0.9 pA/pF (n = 65; Table I). The noninactivating K^+ current component that remains at the end of 4.5-s voltage steps (Fig. 1 B) is referred to here as I_{ss} (steady state). It is important to note that I_{ss} is not the same as the "sustained" K^+ current recently described by Fiset et al. (1998) that was measured at the end of 500-ms voltage steps, and almost certainly reflects the sum of two K^+ currents, $I_{K,slow}$ and I_{ss} (see DISCUSSION). As with $I_{to,f}$ and $I_{K,slow}$, I_{ss} densities varied measurably among cells: at +40 mV, for example, I_{ss} density ranged from 1.7 to 10.5 pA/pF, with a mean ± SEM of 5.5 ± 0.3 pA/pF (n = 65; Table I).

A Novel, Transient K^+ Current in Adult Mouse Ventricular Myocytes Lacking $I_{to,f}$

Analysis of the decay phases of the outward currents evoked during 4.5-s depolarizations in cells lacking $I_{to,f}$ (Fig. 1 D) also revealed two inactivating components with mean ± SEM (n = 7) decay time constants (τ_{decay}) of 196 ± 7 and 1,368 ± 101 ms (Table I); neither time constant displays any appreciable voltage dependence (Fig. 2 B). The τ_{decay} (196 ± 7 ms) for the faster component of current decay in these cells is significantly ($P <$ 0.001) larger than the τ_{decay} (85 ± 2 ms) for $I_{to,f}$. In addition, when all of the fast τ_{decay} values are compared (Fig. 2 C), the cells with a mean ± SEM τ_{decay} of 196 ± 7 ms fall well outside of the otherwise normal distribution of decay time constants. Taken together, these observations suggest a distinct subpopulation of cells (see

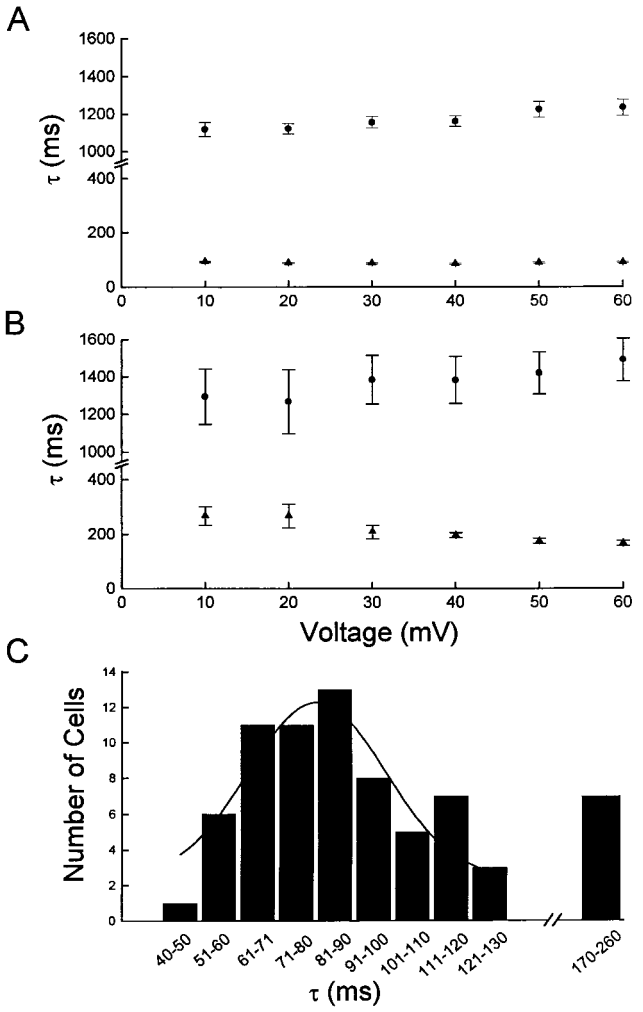

FIGURE 2. Multiple components of inactivation in adult mouse ventricular myocytes. The decay phases of the outward currents, recorded as described in Fig. 1 during 4.5-s depolarizing voltage steps to test potentials between +10 and +60 mV, were fitted using the equation: $y(t) = A_1 * \exp(-t/\tau_1) + A_2 * \exp(-t/\tau_2) + A_{ss}$ (see MATERIALS AND METHODS); time zero was set at the peak of the outward current. Mean ± SEM inactivation time constants for the fast and slow components of inactivation in cells with (A, n = 65) and without (B, n = 7) the rapidly decaying outward K^+ current, $I_{to,f}$, are plotted. As is evident, none of the inactivation time constants displays any appreciable voltage dependence (see text). The mean ± SEM inactivation time constants for the slowly decaying currents ($I_{K,slow}$) are indistinguishable in the two groups of cells, whereas the fast inactivation time constants are significantly ($P <$ 0.001) different (see text). (C) Fast inactivation time constants in the majority of mouse ventricular myocytes (65 of 72) are normally distributed. Inactivation time constants were determined in individual cells from the double exponential fits to the decay phases of the currents and binned (10 ms). The solid line is a simple Gaussian fit to the data points in the majority of the cells (65 of 72); the seven cells lacking $I_{to,f}$ (and with a mean ± SEM τ_{decay} = 196 ± 7 ms) clearly fall outside this normal distribution (see text).

Published May 1, 1999

below), and this current is referred to here as $I_{to,s}$ for transient outward, slow (see below). $I_{to,s}$ density in these cells ranged (at +40 mV) from 4.8 to 16.8 pA/pF, with a mean ± SEM (n = 7) density of 11.4 ± 1.9 pA/pF (Table I). In contrast to the differences in the rates of inactivation of the rapid components (i.e., $I_{to,f}$ and $I_{to,s}$) of current decay, the mean ± SEM τ_{decay} (1,368 ± 101 ms) for the slowly inactivating current in the cells lacking $I_{to,f}$ is not significantly different from the mean ± SEM τ_{decay} for $I_{K,slow}$ (1,162 ± 29 ms) in cells with $I_{to,f}$ (Table I), consistent with the presence of $I_{K,slow}$ in both populations of cells. In addition, the mean ± SEM (n = 7) $I_{K,slow}$ density of 15.6 ± 2.1 pA/pF in cells lacking $I_{to,f}$ (Table I) is not significantly different from the mean ± SEM $I_{K,slow}$ density (of 14.9 ± 0.9 pA/pF) in cells with $I_{to,f}$ (Table I). In cells lacking $I_{to,f}$, however, $I_{K,slow}$ contributes, on average, 50% to the peak outward currents; i.e., substantially more than the average contribution (32%) of this current to the peak in cells with $I_{to,f}$ (Table I). I_{ss} is also evident in adult mouse ventricular myocytes expressing $I_{to,s}$ (Fig. 1 D); I_{ss} density at +40 mV in these cells ranged from 2.5 to 6.2 pA/pF, with a mean ± SEM (n = 7) of 4.5 ± 0.5 pA/pF, a value that is not significantly different from the mean ± SEM I_{ss} density of 5.5 ± 0.3 pA/pF (n = 65) in cells with $I_{to,f}$ (Table I).

The finding of the slowly inactivating, transient outward K^+ current, $I_{to,s}$, in a subset of adult mouse ventricular myocytes prompted us to consider the possibility that this current might also be present in cells with $I_{to,f}$, but simply not be readily detected because the density is too low (particularly relative to $I_{to,f}$) to be resolved. To test this hypothesis, the decay phases of the currents were fitted assuming three exponential components (see MATERIALS AND METHODS) with fixed inactivation time constants of τ_1 = 80 ms (for $I_{to,f}$), τ_2 = 1,200 ms (for $I_{K,slow}$), and τ_3 = 200 ms (for $I_{to,s}$). These analyses revealed that the decay phases of the total outward K^+ currents in some (40 of 65) cells could indeed be fitted by the sum of three exponentials; in the other 25 cells, the fits did not converge or the amplitude of the component with the τ_{decay} = 200 ms was negative. Importantly, even when current records could be fitted to the sum of three exponentials, the quality of the fits was not improved significantly by the inclusion of the third component. Based on these analyses, therefore, it was not possible to determine whether some mouse ventricular cells do indeed express both $I_{to,f}$ and $I_{to,s}$.

Regional Differences in the Expression of $I_{to,f}$ and $I_{to,s}$

The finding of cells expressing $I_{to,s}$ and lacking $I_{to,f}$ prompted us to explore the possibility that there might be regional differences in the expression/densities of these functionally distinct K^+ conductance pathways in mouse ventricle. To test this hypothesis directly, tissue pieces were dissected from the ventricular septum and from the apex of the left ventricle and dispersed (see MATERIALS AND METHODS). Electrophysiological recordings revealed that the waveforms of the outward K^+ currents in left ventricular myocytes isolated from these two regions are indeed distinct (Fig. 3). Peak outward K^+ current densities in cells from the apex (mean ± SEM = 57.2 ± 3.5 pA/pF, n = 35) are significantly ($P < 0.001$) greater than in cells isolated from the septum (mean ± SEM = 28.5 ± 1.5 pA/pF, n = 28; Table II). In addition, for all cells isolated from the apex, analysis of the waveforms of the outward currents evoked during long (4.5 s) depolarizations revealed the presence of $I_{to,f}$, $I_{K,slow}$, and I_{ss} (Table II). The mean ± SEM τ_{decay} for $I_{to,f}$ in these cells was 59 ± 2 ms (n = 35; see DISCUS-

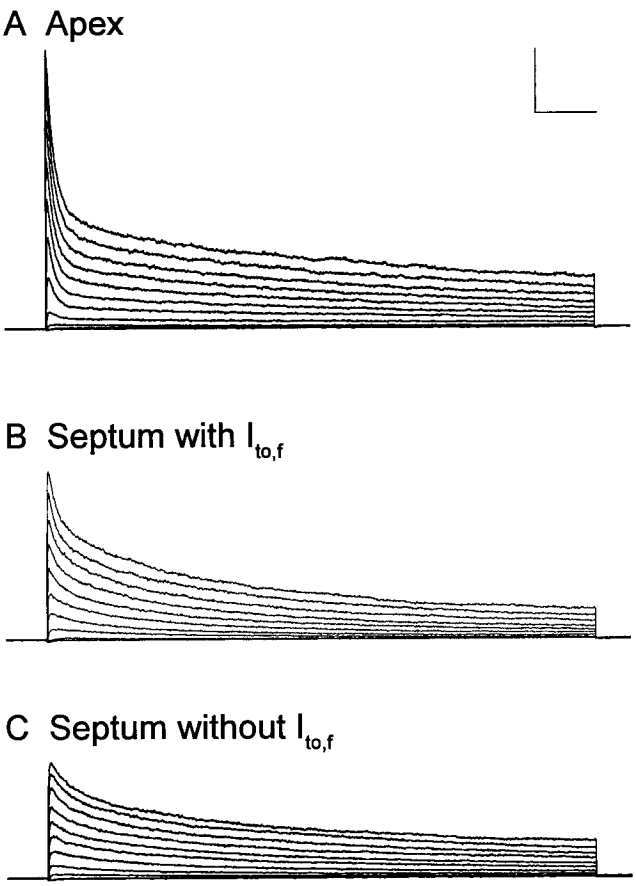

FIGURE 3. Regional differences in Ca^{2+}-independent, depolarization-activated K^+ currents in isolated adult mouse left ventricular myocytes. Outward K^+ currents were recorded as described in Fig. 1 during 4.5-s depolarizing voltage steps to potentials between −40 and +60 mV from a holding potential of −70 mV; the records displayed are from three different cells: one isolated from the apex (A) and the other two from the septum (B and C). As is evident, peak outward current amplitudes in A are substantially larger than those in B and C. In addition, the decay phases of the outward K^+ currents in C are slower than those in A or B and the rapidly inactivating transient K^+ current, $I_{to,f}$ that is so prominent in A is not evident in the records in C (see text). Scale bars, 2 nA and 500 ms.

Published May 1, 1999

table ii

Regional Differences in the Expression of Mouse Ventricular K^+ Currents

Source	I_{peak}	$I_{to,f}$	$I_{to,s}$	$I_{K,slow}$	I_{ss}
Apex					
τ_{decay} (ms)	—	59 ± 2	—	1174 ± 17	—
Density*					
(pA/pF)	57.2 ± 3.5	34.6 ± 2.6	—	17.2 ± 1.1	5.5 ± 0.4
Percent I_{peak}	—	60	—	30	10
n	35	35	—	35	35
Septum					
Cells with $I_{to,f}$					
τ_{decay} (ms)	—	53 ± 2	258 ± 15	1180 ± 45	—
Density*					
(pA/pF)	30.9 ± 1.5	6.8 ± 0.5	7.4 ± 0.7	12.5 ± 0.6	4.3 ± 0.3
Percent I_{peak}	—	22	24	40	14
n	22	22	22	22	22
Cells lacking $I_{to,f}$					
τ_{decay} (ms)	—	—	194 ± 11	1143 ± 64	NA
Density*					
(pA/pF)	20.5 ± 2.5	—	5.4 ± 0.9	10.4 ± 1.5	4.8 ± 0.4
Percent I_{peak}	—	—	26	51	23
n	6	—	6	6	6

*Current densities were determined from analyses of records obtained on depolarization to +40 mV from a holding potential of −70 mV; all values are means ± SEM.

sion); $I_{to,f}$ density (at +40 mV) in these cells ranged from 13.8 to 79.5 pA/pF, with a mean ± SEM (n = 35) density of 34.6 ± 2.6 pA/pF and, on average, $I_{to,f}$ contributes 60% to the peak outward K^+ currents in apex cells (Table II). Mean ± SEM (n = 35) $I_{K,slow}$ and I_{ss} densities at +40 mV in these cells were 17.2 ± 1.1 and 5.5 ± 0.4 pA/pF (Table II).

(Fig. 3) The waveforms of the outward K^+ currents in cells isolated from the septum appear different and are more variable than those seen in cells from the apex. Two distinct outward K^+ current waveforms were recorded in cells isolated from the septum (Fig. 3, B and C). Some cells, for example, clearly lack $I_{to,f}$ (Fig. 3 C), and analyses of the decay phases of the currents in these cells revealed two components with τ_{decay} of 194 ± 11 and 1,143 ± 64 ms (Table II). These values are indistinguishable for those determined above for $I_{to,s}$ and $I_{K,slow}$ (Table I). $I_{to,s}$ density (at +40 mV) ranged from 2.8 to 8.5 pA/pF, with a mean ± SEM (n = 6) density of 5.4 ± 0.9 pA/pF (Table II) and, on average, $I_{to,s}$ contributes 26% to the peak outward K^+ currents in these cells (Table II). The mean ± SEM $I_{K,slow}$ density (10.4 ± 1.5 pA/pF) in septum cells lacking $I_{to,f}$ (Table II) is similar to the density of this current component in cells with $I_{to,f}$ (Tables I and II). In cells lacking $I_{to,f}$, however, $I_{K,slow}$ contributes, on average, ≈50% to the peak outward currents; i.e., substantially more than the average contribution (of 30–40%) seen in cells with $I_{to,f}$ (Tables I and II). In the other subset of cells from the septum (Fig. 3 B), three exponentials with mean ± SEM (n = 22) time constants of 53 ± 2, 258 ± 15, and 1,180 ± 45 ms were required to fit the decay phases of the currents; the decay time constants for these three components suggest the coexpression of $I_{to,f}$, $I_{to,s}$, and $I_{K,slow}$ (as well as I_{ss}; Table II). The mean ± SEM $I_{to,f}$ density in these cells (6.8 ± 0.5 pA/pF at +40 mV, n = 22) in these cells is significantly lower ($P < 0.001$) than the mean ± SEM $I_{to,f}$ density (34.6 ± 2.6 pA/pF at +40 mV, n = 35) in cells from the left ventricular apex, and $I_{to,f}$ only contributes ~20% to the peak outward currents in these cells, compared with 60% in apex cells (Table II). In addition, the densities of $I_{K,slow}$ and I_{ss} in cells isolated from the septum are slightly lower than in apex cells. I_{ss} density at +40 mV in these cells ranged from 2.5 to 6.2 pA/pF, with a mean ± SEM (n = 7) of 4.5 ± 0.5 pA/pF. Also, in septum cells, I_{ss} contributes significantly more to the total outward current than does I_{ss} in apex cells (Table II).

Pharmacological Separation of the K^+ Currents in Adult Mouse Ventricular Myocytes

Subsequent experiments were focussed on examining the pharmacological sensitivities of the outward K^+ currents in adult mouse ventricular myocytes and on determining if the kinetically distinct K^+ current components could also be distinguished pharmacologically. In initial experiments, the effects of varying concentrations (10 μM to 5 mM) of 4-AP on whole-cell K^+ currents were examined. Control K^+ currents, evoked during 500-ms and 4.5-s voltage steps, were recorded before superfusion of 4-AP–containing bath solutions and, when the effect of 4-AP had reached a steady state, outward currents were again recorded. To obtain the current(s) blocked by 4-AP, records obtained in the presence of each concentration of 4-AP were digitally subtracted from the controls. Examples of typical experiments and the currents blocked by varying concentrations of 4-AP are presented in Fig. 4. The currents blocked by 10 μM 4-AP activate rapidly and inactivate slowly (Fig. 4 C). Analysis of the decay phases of the 10 μM 4-AP–sensitive currents suggests that $I_{K,slow}$ is selectively attenuated (by ≈35%), consistent with previous reports of the 4-AP sensitivity of this conductance pathway (Fiset et al., 1998; London et al., 1998a). In the presence of 50 μM 4-AP, $I_{K,slow}$ is further reduced to <50% of control (n = 7), whereas $I_{to,f}$ is slightly (≈16%) reduced, and I_{ss} is unaffected (Table III).

Exposure of adult mouse ventricular myocytes to concentrations of 4-AP > 100 μM also blocks $I_{to,f}$ (Table III). After application of 0.5 mM 4-AP, for example, peak outward currents are attenuated markedly (Fig. 4 E), and comparison of the control currents (Fig. 4 D) and the currents blocked by 0.5 mM 4-AP (Fig. 4 F) re-

Published May 1, 1999

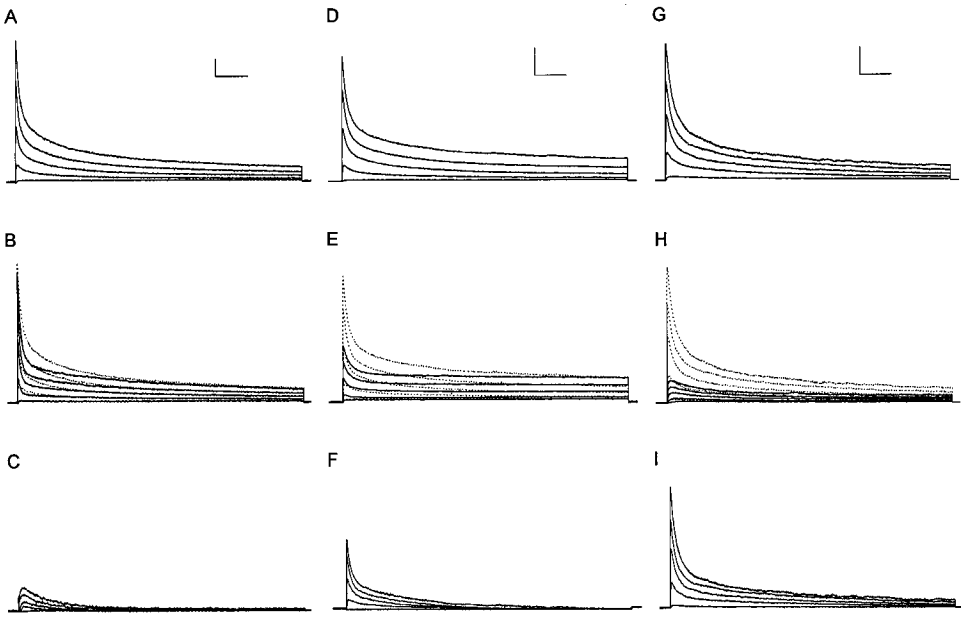

FIGURE 4. Effects of varying concentrations of 4-AP on adult mouse ventricular K^+ currents. Outward K^+ currents were recorded as described in Fig. 1 during 4.5-s depolarizing voltage steps to −20 to +60 mV from a holding potential of −70 mV; records from three cells exposed to different concentrations (10 μM, 0.5 mM, and 5 mM) of 4-AP are presented. In each example, control currents (A, D, and G) were recorded before application of 4-AP; cells were the exposed to (10 μM, 0.5 mM, or 5 mM) 4-AP, and when the effect (of 4-AP) reached steady state, the currents in the presence of 10 μM (B), 0.5 mM (E), and 5 mM (H) 4-AP were recorded. In B, E, and H, the currents in the presence of 4-AP are plotted as solid lines, and the control records (A, D, and G, respectively) are replotted as points to facilitate comparison. The waveforms of the 10 μM (C), 0.5 mM (F), and 5 mM (I) 4-AP–sensitive currents were obtained by off-line digital subtraction of the currents in the presence of 4-AP from the controls. For each 4-AP concentration, similar results were obtained in experiments on four cells. Scale bars, 2 nA and 500 ms.

vealed that $I_{K,slow}$ is blocked by ≈80% and $I_{to,f}$ is reduced by ≈50% at 0.5 mM 4-AP; I_{ss}, in contrast, is unaffected by 0.5 mM 4-AP (Table III). When the 4-AP concentration is increased to 5 mM, outward currents are markedly reduced (Fig. 4 H), and analysis of the control (Fig. 4 G) and the 5 mM 4-AP–sensitive (Fig. 4 I) currents revealed that $I_{to,f}$ (as well as $I_{K,slow}$) is blocked completely at this (5 mM) 4-AP concentration. The currents remaining in 5 mM 4-AP (Fig. 4 H) are interpreted as reflecting only I_{ss}, although I_{ss} is attenuated by ≈35% at high concentrations of 4-AP (Table III). Experiments conducted on mouse ventricular myocytes isolated from the septum reveal that $I_{to,s}$ is also blocked by 4-AP (Fig. 5; Table III). Application of 10 μM 4-AP to septum cells selectively attenuates $I_{K,slow}$ (Fig. 5, B and C), and higher concentrations of 4-AP are required to also affect $I_{to,s}$ (Fig. 5, D and E). In the presence of 0.5 mM 4-AP, $I_{to,s}$ is attenuated by ≈70% and $I_{K,slow}$ is blocked completely (Table III; Fig. 5).

To test the validity of the separation of the currents based on differential sensitivities to 4-AP (Figs. 4 and 5), the effects of varying concentrations of other K^+ channel blockers, TEA, α-DTX, and HpTx-3 were also examined. As in the experiments with 4-AP, outward K^+ currents were recorded before and after bath applications of these blockers, and the drug-sensitive currents were obtained by off-line digital subtraction of these records. (Fig. 6 B) Exposure to 25 mM TEA resulted in marked attenuation of the peak currents and the currents remaining at the end of long depolarizing voltage steps. Analysis of the 25 mM TEA-sensitive currents (Fig. 6 C) reveals that these currents activate rapidly and inactivate slowly to a steady state level. The decay phases of the 25 mM TEA-sensitive currents were well described by single exponential with a mean ± SEM τ_{decay} of 1,234 ± 197 ms (n = 4), a value that is similar to the τ_{decay} of $I_{K,slow}$ (Tables I and II). In addition, comparison of the current waveforms in Fig. 6 B reveals that both I_{ss} and $I_{K,slow}$ are reduced by ≈60% at this TEA concentration, whereas $I_{to,f}$ is unaffected (Table III). In similar experiments completed on cells isolated from the septum, $I_{to,s}$ is also found to be unaffected by 25 mM TEA (Table III). When the TEA concentration was in-

TABLE III

*Pharmacological Profiles of Mouse Ventricular K^+ Currents**

Drug	$I_{to,f}$	n	$I_{to,s}$	n	$I_{K,slow}$	n	I_{ss}	n
4-AP (10 μM)	No effect	4	No effect	1	34 ± 7%	4	No effect	4
4-AP (50 μM)	16 ± 2%	7	ND		49 ± 5%	7	No effect	7
4-AP (0.5 mM)	54 ± 5%	5	81 ± 1%	3	78 ± 4%	5	No effect	5
4-AP (5 mM)	100%	4	100%	4	100%	4	38 ± 2%	4
TEA (25 mM)	No effect	4	No effect	4	58 ± 4%	4	58 ± 5%	4
TEA (135 mM)	46 ± 5%	4	ND		100%	4	61 ± 6%	4
HpTx-3 (100 nM)	34 ± 1%	3	No effect	3	No effect	3	No effect	4
HpTx-3 (300 nM)	100%	1	No effect	1	No effect	1	No effect	1

*Values represent percent block of the component current amplitude evoked on depolarizations from −70 to +40 mV from a holding potential of −70 mV; values are means ± SEM.

Published May 1, 1999

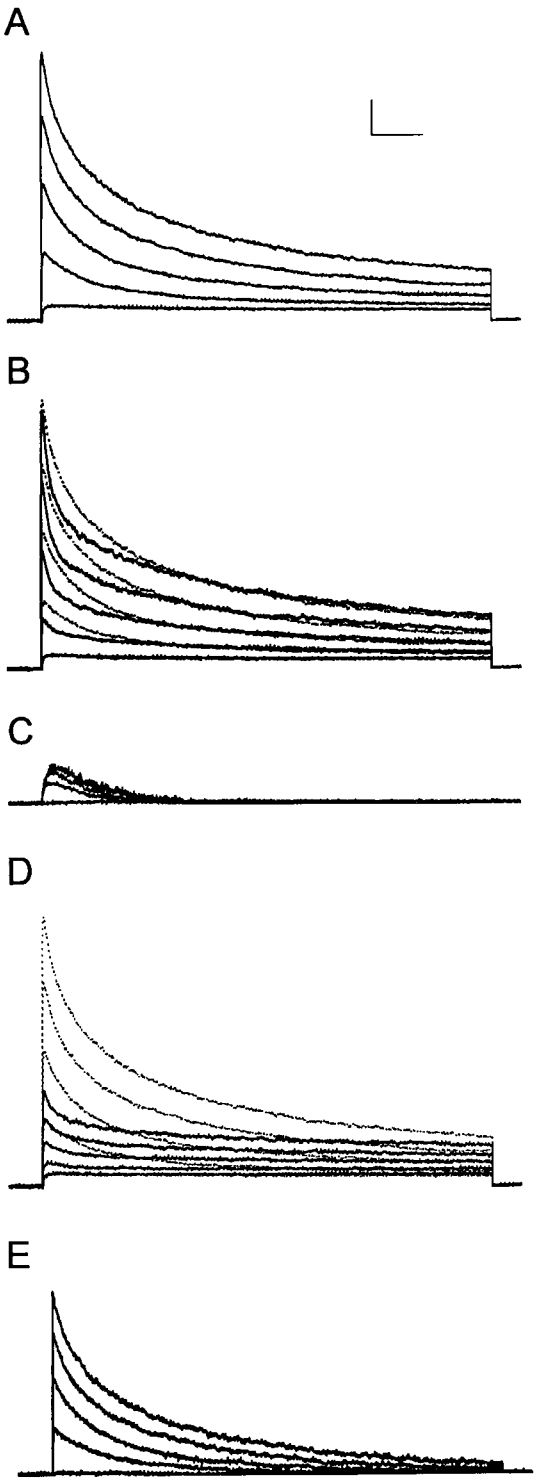

FIGURE 5. $I_{to,s}$ is blocked by high (0.5 mM), but not by low (10 μM), concentrations of 4-AP. Outward K^+ currents were recorded from a cell isolated from the septum as described in Fig. 1 during 4.5-s depolarizing voltage steps from −30 to +60 mV from a holding potential of −70 mV; all of the records displayed are from the same cell. Control currents (A) and currents in the presence of 10 μM (B) or 0.5 mM (D) 4-AP were recorded. In B and D, the currents recorded in the presence of 10 μM (B) and 0.5 mM (D) 4-AP are plotted as solid lines, and the control records (in the absence of 4-AP, A) are replotted as points to facilitate comparison. The waveforms of the 10 μM (C) and 0.5 mM (E) 4-AP–sensitive currents were obtained by off-line digital subtraction of the current records in the presence of 10 μM (B) or 0.5 mM (D) 4-AP from the controls (A). Similar results were obtained in experiments on four septum cells. Scale bars, 1 nA and 500 ms.

creased to 135 mM, the currents remaining are rapidly inactivating (Fig. 6 E). Both I_{ss} and $I_{K,slow}$ are blocked completely and $I_{to,f}$ is blocked by ≈40% by isotonic TEA (Table III).

In experiments completed with α-DTX at concentrations up to 100 nM (n = 4), no measurable effects on the outward K^+ currents in adult mouse ventricular myocytes were observed (not shown). In contrast, local applications of 100–300 nM HpTx-3 resulted in the selective attenuation of $I_{to,f}$ (Fig. 7). In cells isolated from the apex of the left ventricle, for example, 100 nM HpTx-3 reduced $I_{to,f}$ by 30–40% (Fig. 7, left). In cells isolated from the septum that express $I_{to,f}$, this current is selectively attenuated by HpTx-3 (Fig. 7, middle), whereas $I_{to,s}$ in cells with (Fig. 7, middle) and without (Fig. 7, right) $I_{to,f}$ is unaffected by HpTx-3 at concentrations up to 300 nM.

Voltage Dependences and Kinetics of Activation of $I_{to,f}$, $I_{to,s}$, $I_{K,slow}$, and I_{ss}

Having identified four distinct depolarization-activated K^+ currents, $I_{to,f}$, $I_{to,s}$, $I_{K,slow}$, and I_{ss}, in adult mouse ventricular myocytes, subsequent experiments were focussed on characterizing the time- and voltage-dependent properties of these currents. For most of these analyses, the amplitudes of the currents were determined from exponential fits to the decay phases of the currents evoked during long depolarizing voltage steps. In some cases, the individual current components, separated based on differential sensitivities to 4-AP and TEA, were also analyzed. In the pharmacological analyses, $I_{K,slow}$ was defined as the 10-μM 4-AP–sensitive current (Fig. 4 C); the current remaining in the presence of 5 mM 4-AP (Fig. 4 H) was analyzed as I_{ss}, and the current remaining in 135 mM TEA (Fig. 6 E) was analyzed as $I_{to,f}$. Most of the initial experiments were completed on randomly dispersed adult mouse ventricular myocytes; detailed analysis of $I_{to,s}$ was completed on cells isolated from the septum. In some cases, the properties of $I_{to,f}$, $I_{K,slow}$, and I_{ss} in apex and septum cells were determined and compared. To examine the voltage dependences of activation, the amplitudes of the individual current components at each test potential (in each cell) were measured and normalized to the current amplitude determined (in the same cell) at +30 mV; mean normalized currents are plotted as a function of test potential in Fig. 8 A. Although the voltage depen-

Published May 1, 1999

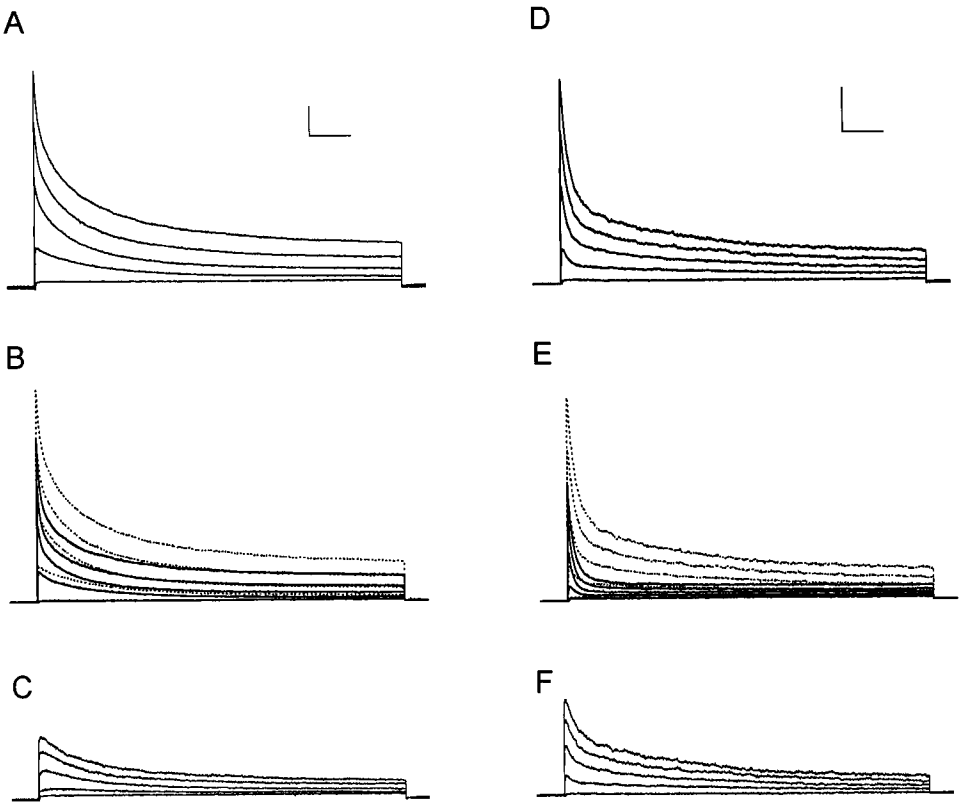

FIGURE 6. TEA blocks $I_{K,slow}$ and I_{ss} in adult mouse ventricular myocytes. Outward currents were recorded as described in Fig. 1 during 4.5-s depolarizing voltage steps to −20 to +60 mV from a holding potential of −70 mV; records from two cells exposed to 25 (A–C) or 135 (D–F) mM are presented. In each example, control currents (A and D) were recorded before application of TEA; cells were the exposed to 25 or 135 mM TEA, and when the effect (of TEA) reached steady state, the currents in the presence of 25 (B) or 135 (E) mM TEA were recorded. In B and E, the currents in the presence of 4-AP are plotted as solid lines, and the control records (A and D, respectively) are replotted as points to facilitate comparison. The waveforms of the 25-mM (C) and 135-mM (F) TEA-sensitive currents were obtained by off-line digital subtraction of the currents in the presence of TEA from the controls. Similar results were obtained in experiments on three (25 mM TEA) or four (135 mM TEA) cells. Scale bars, 2 nA and 500 ms.

dences of activation of $I_{to,f}$, $I_{to,s}$, $I_{K,slow}$, and I_{ss} are similar in that the currents begin to activate at less than −30 mV, the foot of the current–voltage plot for $I_{to,f}$ is less steep than for $I_{to,s}$, $I_{K,slow}$, or I_{ss} (Fig. 8 A).

Time constants of activation for $I_{to,f}$, $I_{K,slow}$, and I_{ss} were determined from single exponential fits to the rising phases of the currents separated using 4-AP and TEA. For these analyses, $I_{K,slow}$ was defined as the 10 μM 4-AP–sensitive current (Fig. 4 C), and $I_{to,f}$ and I_{ss} were defined as the currents remaining in the presence of 135 mM TEA (Fig. 6 E) or 5 mM 4-AP (Fig. 4 H), respectively. For all current components, the rising phases of the currents at each test potential were well described by single exponentials. Mean (± SEM) activation time constants for $I_{to,f}$, $I_{K,slow}$, and I_{ss} are plotted as a function of test potential in Fig. 8 B. As is evident, $I_{to,f}$ and $I_{K,slow}$ activate rapidly, and with similar activation time constants. I_{ss}, in contrast, activates much more slowly than either $I_{to,f}$ or $I_{K,slow}$ at all test potentials (Fig. 8 B). In addition, analyses of the rising phases of the currents in records such as those in Figs. 4 C and 6 C revealed that the time constants of activation of the 25-mM TEA-sensitive currents and 10-μM 4-AP–sensitive currents are indistinguishable: mean ± SEM activation time constants at +40 mV for the 25-mM TEA-sensitive currents (Fig. 6 C) and the 10-μM 4-AP–sensitive currents (Fig. 4 C), for example, are 1.9 ± 0.5 ms (n = 4) and 2.1 ± 0.2 ms (n = 4), respectively. $I_{K,slow}$, therefore, is blocked selectively by both 10 μM 4-AP and 25 mM TEA.

The activation time constants (tau, τ) are voltage dependent, decreasing with increasing depolarization, and the variations with voltage are well described by single exponential functions of the form: $\tau(V) = a + b\,[\exp(-V_m/c)]$, where V_m is the test potential and c is a constant that defines the steepness of the voltage dependence. The best fits (Fig. 8 B, continuous lines) to the data yielded: c = 27.1 (a, 0.54; b, 11.2) for $I_{to,f}$; c = 18.1 (a, 1.1; b, 10.1) for $I_{K,slow}$; and c = 13.0 (a, 12.5; b, 3.9) for I_{ss}. Comparison of the c values derived from these fits indicates that $I_{to,f}$ and $I_{K,slow}$ activation rates vary similarly as a function of voltage, whereas the voltage dependence of I_{ss} activation is much steeper (Fig. 8 B).

Voltage Dependences of Steady State Inactivation of $I_{to,f}$, $I_{to,s}$, and $I_{K,slow}$

The voltage dependences of steady state inactivation of $I_{to,f}$, $I_{to,s}$, and $I_{K,slow}$ were examined during voltage steps

Published May 1, 1999

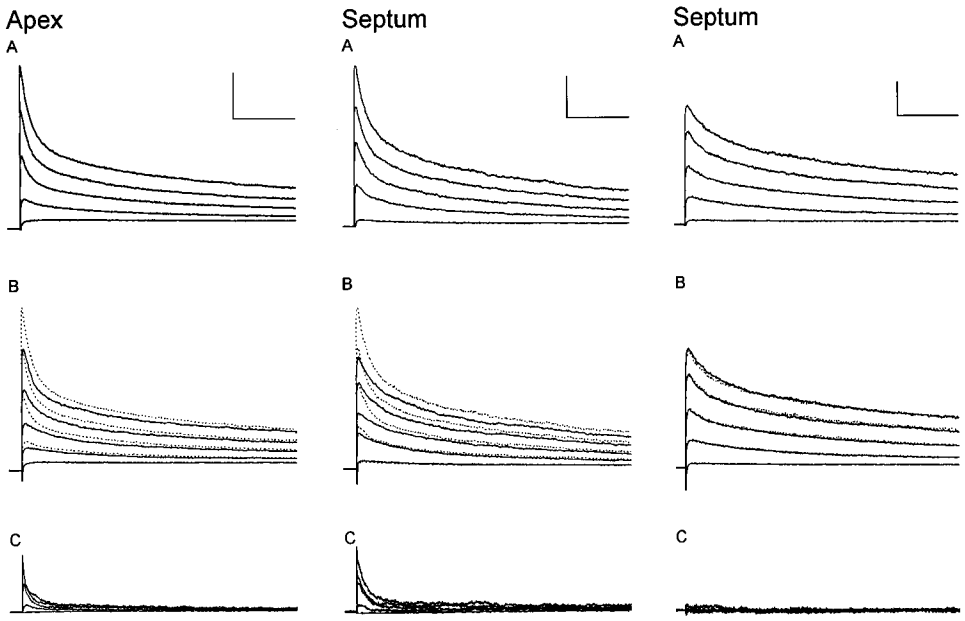

FIGURE 7. $I_{to,f}$ is selectively blocked by HpTx-3. Outward currents were recorded in mouse ventricular myocytes isolated from the apex and septum as described in Fig. 1 during 4.5-s depolarizing voltage steps to potentials between −20 and +60 mV from a holding potential of −70 mV; A–C in each panel were obtained from the same cell. In each cell, control currents (A) were recorded before exposure to 100 or 300 nM HpTx-3; outward K^+ currents were again recorded after the effect of HpTx-3 reached a steady state (B). (B) The currents in the presence of HpTx-3 are plotted as solid lines, and the control records (A) are replotted as points to facilitate comparison. Off-line digital subtraction of the currents in the presence of HpTx-3 (B) from the controls (A) revealed that only the rapidly inactivating K^+ current, $I_{to,f}$, in apex and septum cells is affected by HpTx-3 (C). Similar results were obtained in experiments on four cells. Scale bars, 2 nA and 500 ms.

to +50 mV presented after 5-s conditioning prepulses to potentials between −100 and −10 mV; the protocol is shown below the current records in Fig. 9. Experiments were completed on randomly selected myocytes, as well as on cells isolated from the left ventricular apex (Fig. 9 A) and septum (B). In the first two cases, the decay phases of the currents evoked at +50 mV from each prepulse potential were fitted to the sum of two exponentials to provide $I_{to,f}$ and $I_{K,slow}$. For cells isolated from the septum, the amplitudes of $I_{to,s}$, $I_{to,f}$ (when present) and $I_{K,slow}$ were determined from (double or triple) exponential fits to the decay phases of the currents evoked at +50 mV from each prepulse potential. The amplitudes of $I_{to,f}$, $I_{to,s}$, and $I_{K,slow}$ evoked from each conditioning potential were then normalized to their respective maximal current amplitudes (in the same cell) evoked from −100 mV. Mean (± SEM) normalized $I_{to,f}$, $I_{to,s}$, and $I_{K,slow}$ amplitudes are plotted as a function of conditioning potential in Fig. 9 C; the continuous lines represent the best Boltzmann fits to the averaged data.

The steady state inactivation data for I_{to} are well described by single Boltzmann with a $V_{1/2}$ of −24 mV (k = 3.8 mV; Fig. 9 C). For $I_{to,s}$ and $I_{K,slow}$, in contrast, the variations in current amplitudes with conditioning voltage were not well described by a single Boltzmann, and two Boltzmanns were required to fit the data (Fig. 9 C). For $I_{K,slow}$, the $V_{1/2}$ values derived from these fits were −73 mV (k = 6.7 mV) and −19 mV (k = 6.0 mV), and for $I_{to,s}$, the $V_{1/2}$ values were −64 mV (k = 9.0 mV) and −19 mV (k = 6.3 mV). The voltage dependences of steady state inactivation of $I_{to,s}$ and $I_{K,slow}$ are very similar (Fig. 9 C), both in terms of the steepness (k values) of the curves and the relative amplitudes (≈35%, $V_{1/2}$ = −73 mV, and ≈65%, $V_{1/2}$ = −19 mV) of the two components. The finding of two components of steady state inactivation suggest the presence of two populations of channels contributing to $I_{K,slow}$ (and $I_{to,s}$) or, alternatively, the complex gating of a single population of $I_{K,slow}$ ($I_{to,s}$) channels (see DISCUSSION).

Recovery of $I_{to,f}$, $I_{to,s}$, and $I_{K,slow}$ from Steady State Inactivation

To examine the time dependences of recovery from steady state inactivation of $I_{to,f}$, $I_{to,s}$, and $I_{K,slow}$, cells were first depolarized to +50 mV for 9.5 s to inactivate the currents (longer depolarizations did not lead to further inactivation), subsequently hyperpolarized to −70 mV for varying times ranging from 10 to 9,064 ms, and finally stepped to +50 mV (to activate the currents and assess the extent of recovery); the protocol is illustrated in Fig. 10. Experiments were completed on randomly selected myocytes, as well as on cells isolated from the left ventricular apex (Fig. 10 A) and septum (B). Typical records obtained from cells isolated from the apex and septum are illustrated in Fig. 10, A and B. For the randomly selected and the apex cells, the decay phases of the currents evoked at +50 mV after each recovery period were fitted to the sum of two exponentials to provide $I_{to,f}$ and $I_{K,slow}$. For cells isolated from the septum, the amplitudes of $I_{to,s}$, $I_{to,f}$ (when present), and $I_{K,slow}$ were determined from (double or triple) expo-

Published May 1, 1999

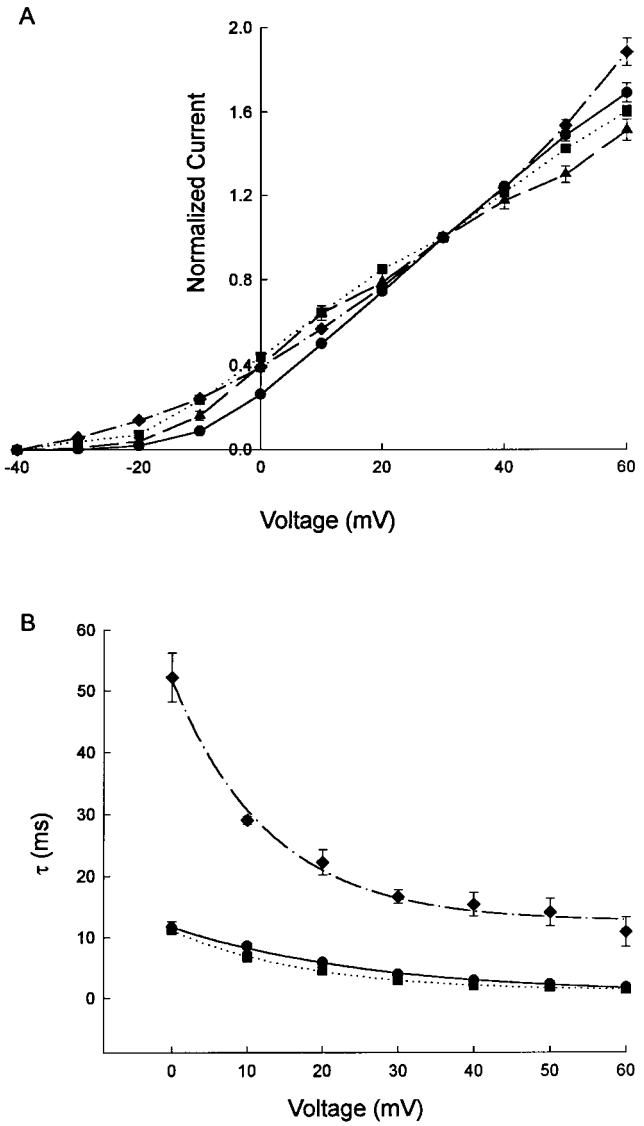

FIGURE 8. $I_{to,f}$, $I_{to,s}$, $I_{K,slow}$, and I_{ss} display similar voltage dependences (A), but different rates (B) of activation. (A) Outward currents were recorded as described in Fig. 1 during 4.5-s depolarizing voltage steps to potentials between −40 and +60 mV from a holding potential of −70 mV. The amplitudes of $I_{to,f}$, $I_{to,s}$, $I_{K,slow}$, and I_{ss} at each test potential in each cell were determined from exponential fits to the decay phases of the total outward currents (see text), normalized to the current amplitude at +60 mV (in the same cell), and mean ± SEM normalized $I_{to,f}$ (●), $I_{to,s}$ (▲), $I_{K,slow}$ (■), and I_{ss} (◆) are plotted (A) as a function of test potential. (B) Activation time constants were determined from single exponential fits to the rising phases of the separated outward K^+ currents (see text) evoked during depolarizing voltage steps from 0 to +60 mV. (B) Mean ± SEM activation time constants for $I_{to,f}$ (●), $I_{K,slow}$ (■), and I_{ss} (◆) are plotted (as points) as a function of test potential. The solid lines represent the best single exponential fits to the data points (see text).

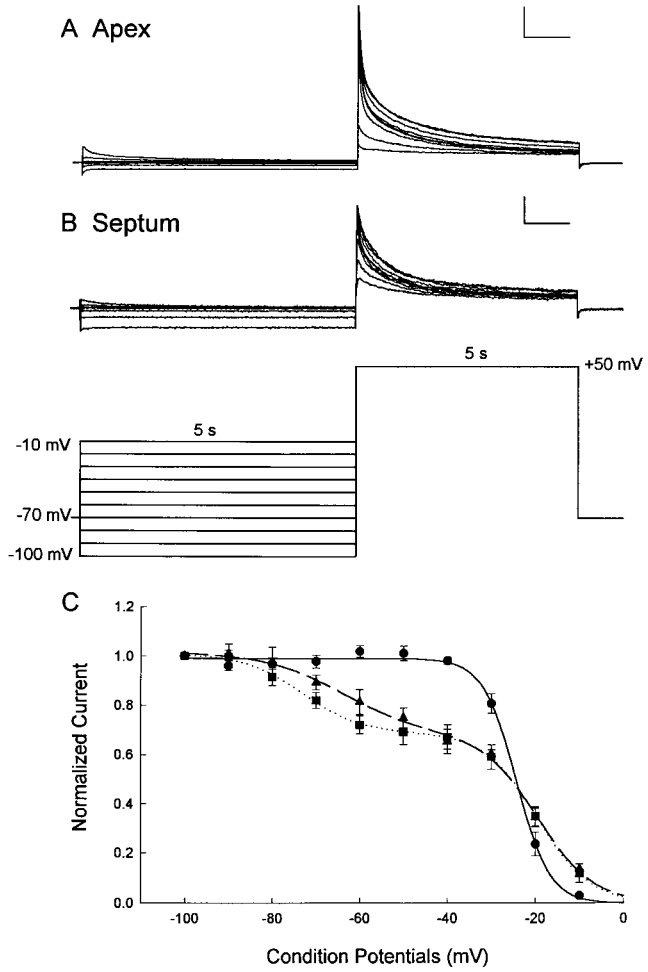

FIGURE 9. Voltage dependences of steady state inactivation of $I_{to,f}$, $I_{to,s}$, and $I_{K,slow}$. To examine the voltage dependences of steady state inactivation, outward K^+ currents evoked during 5-s depolarizations to +50 mV after 5-s conditioning prepulses to potentials between −100 and −10 mV were recorded in mouse myocytes isolated from the apex (A) and septum (B) of the left ventricle; the protocol is illustrated below the current records. The amplitudes of $I_{to,f}$, $I_{to,s}$, and $I_{K,slow}$ evoked at +50 mV from each conditioning potential were determined from double (or triple) exponential fits to the decay phases of the total outward currents (see text), and these values were normalized to the current amplitudes evoked from −100 mV (in the same cell). Mean ± SEM (n = 7) normalized $I_{to,f}$ (●), $I_{to,s}$ (▲), and $I_{K,slow}$ (●) amplitudes were then determined and are plotted as a function of conditioning potential in C. The solid lines reflect the best single ($I_{to,f}$) or double ($I_{to,s}$ and $I_{K,slow}$) Boltzmann fits to the mean normalized data (see text). The scale bars, (A and B) 2 nA and 1 s.

nential fits to the decay phases of the currents evoked at +50 mV after each recovery period; note that for the cell illustrated in Fig. 10 B, $I_{to,f}$ (as well as $I_{to,s}$) is present. The amplitudes of $I_{to,f}$, $I_{to,s}$, and $I_{K,slow}$ after each recovery period were then normalized to their respective maximal current amplitudes (in the same cell) evoked after the 9.5-s recovery time. Mean (± SEM) normalized $I_{to,f}$, $I_{to,s}$, and $I_{K,slow}$ amplitudes are plotted as a function of recovery time in Fig. 10 C; the continuous lines represent the best single exponential fits to the averaged data.

Published May 1, 1999

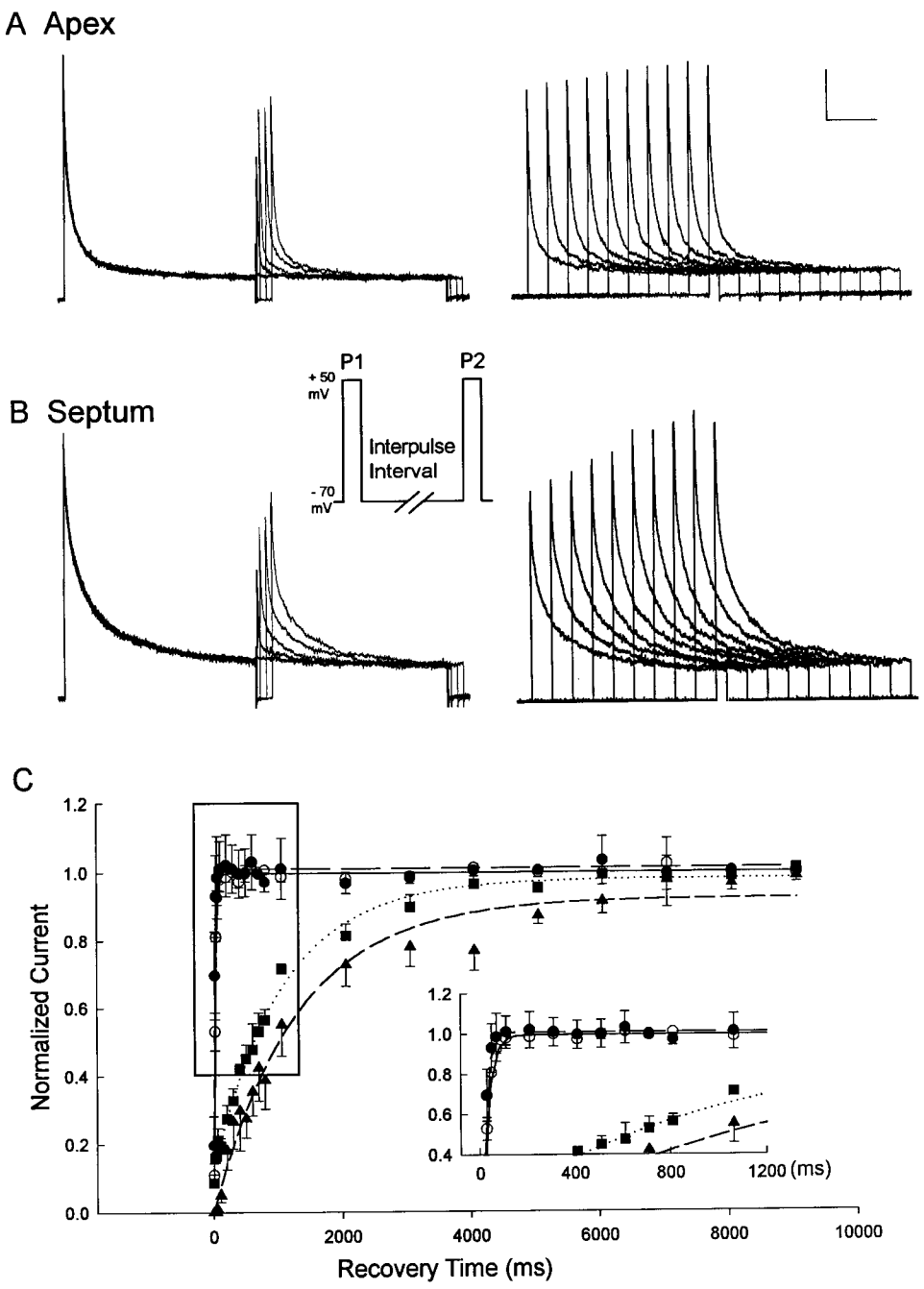

FIGURE 10. The rates of recovery of $I_{to,f}$, $I_{to,s}$, and $I_{K,slow}$ from steady state inactivation are distinct. After inactivating the currents during 9.5-s prepulses to +50 mV, cells were hyperpolarized to −70 mV for times ranging from 0 ms to 10 s before a second (test) depolarization to +50 mV (to assess the extent of recovery); the experimental protocol is illustrated between the records. Typical current waveforms recorded in cells isolated from the apex (A) and septum (B) during the +50-mV conditioning step and the +50-mV test depolarization after varying recovery times are displayed. Currents recorded after brief (10–190 ms) recovery periods are displayed on the left and typical currents seen after longer recovery times (250–1,090 ms) are on the right in A and B. The amplitudes of $I_{to,f}$, $I_{to,s}$, and $I_{K,slow}$ evoked at +50 mV after each recovery period were determined from double (or triple) exponential fits to the decay phases of the total outward currents (see text), and normalized to the current amplitudes evoked after the 10-s recovery period (in the same cell). Mean ± SEM normalized recovery data for $I_{to,f}$ (●, ○), $I_{to,s}$ (▲), and $I_{K,slow}$ (■) are plotted in C; the initial phase of recovery of the currents is shown on an expanded time scale (inset). The two sets of $I_{to,f}$ data were obtained from cells isolated from the apex (●) and septum (○) and, as is evident, recovery of $I_{to,f}$ in the two cells types is indistinguishable. The mean ± SEM (n = 9) normalized recovery data for $I_{to,f}$ (●, ○), $I_{to,s}$ (▲), and $I_{K,slow}$ (■) are well described by a single exponential (see text). Scale bars, (A and B) 500 pA and 2.5 s.

The mean normalized recovery data for $I_{to,f}$ (in left ventricular apex and septum cells) are well described by a single exponential characterized by a time constant of 27 ms (Fig. 10 C, solid line); note that the recovery data for cells isolated from the septum and apex are indistinguishable. The mean normalized recovery data for $I_{to,s}$ and $I_{K,slow}$ also follow a monoexponential time course (Fig. 10 C), and the recovery data are well described by single exponentials with time constants of 1,298 ($I_{to,s}$) and 1,079 ($I_{K,slow}$) ms. Thus, in addition to differences in inactivation rates, $I_{to,f}$ and $I_{to,s}$ also recover from steady state inactivation at markedly different rates (Fig. 10 C).

discussion

Multiple Depolarization-activated K^+ Currents in Adult Mouse Ventricular Myocytes

The results presented here demonstrate the presence of four kinetically and pharmacologically distinct Ca^{2+}-

Published May 1, 1999

independent, voltage-gated K^+ currents in isolated adult mouse ventricular myocytes: $I_{to,f}$, $I_{to,s}$, $I_{K,slow}$, and I_{ss}. Although $I_{K,slow}$ and I_{ss} were found in all ($n = 132$) adult mouse ventricular myocytes studied, $I_{to,f}$ and $I_{to,s}$ were not. In randomly selected mouse ventricular cells, $I_{to,f}$ was evident in the majority (65 of 72, ≈90%) of the cells, whereas $I_{to,s}$ was identified in only 7 of 72 (≈10%) cells; i.e., the 7 cells lacking $I_{to,f}$. Importantly, the densities and the properties of $I_{K,slow}$ and I_{ss} in $I_{to,s}$-expressing cells were indistinguishable from the corresponding currents in cells with $I_{to,f}$. Subsequent experiments revealed regional differences in $I_{to,f}$ and $I_{to,s}$ expression in mouse left ventricles: $I_{to,f}$ was identified in all cells ($n = 35$) isolated from the apex and $I_{to,s}$ was not detected in these cells ($n = 35$); in the septum, by contrast, all cells expressed $I_{to,s}$ ($n = 28$), and in the majority (22 of 28, 80%) of cells, $I_{to,f}$ was also present. The density of $I_{to,f}$ (mean ± SEM at +40 mV = 6.8 ± 0.5 pA/pF, $n = 22$) in septum cells, however, is significantly ($P < 0.001$) lower than $I_{to,f}$ density in cells from the apex (mean ± SEM at +40 mV = 34.6 ± 2.6 pA/pF, $n = 35$). In addition to differences in inactivation kinetics, $I_{to,f}$, $I_{to,s}$, and $I_{K,slow}$ were also distinguished here by marked differences in the rates of recovery (from inactivation), as well as differential sensitivities to 4-AP, TEA, and HpTx-3; none of the currents in mouse ventricular myocytes was found to be sensitive to the dendrotoxins.

The absolute amplitudes of the individual current components varied among cells and, in all randomly selected cells with $I_{to,f}$ ($n = 65$) and in cells from the apex ($n = 35$), the density of I_{ss} was substantially less than the density of either $I_{to,f}$ or $I_{K,slow}$ (Tables I and II). On average, the ratio of current densities in these (randomly selected and apex) cells was 5–6:3:1 for $I_{to,f}$, $I_{K,slow}$, and I_{ss}, respectively. In the $I_{to,s}$-expressing cells from the septum, peak outward K^+ current densities are significantly ($P < 0.001$) lower (in cells with and without $I_{to,f}$) than the peak outward current density in cells from the apex (Table II), although no differences in cell sizes or input resistances were evident when these two groups of cells were compared. The mean ± SEM $I_{K,slow}$ density is also significantly ($P < 0.001$) lower in septum than in apex cells (Table II). There were no significant differences, however, in mean ± SEM I_{ss} densities among the various populations of adult mouse ventricular (i.e., randomly selected) cells from the apex or cells from the septum (both the cells with and without $I_{to,f}$; Tables I and II). On average, the ratio of current densities in $I_{to,s}$-expressing cells was 1:2:1 for $I_{to,s}$, $I_{K,slow}$, and I_{ss}, respectively, in cells lacking $I_{to,f}$ and 1:1:2:0.7 for $I_{to,f}$, $I_{to,s}$, $I_{K,slow}$, and I_{ss}, respectively, for the cells with $I_{to,f}$ (Table II).

Functionally, $I_{to,f}$, $I_{to,s}$, and $I_{K,slow}$ underlie the peak outward currents in all mouse ventricular cells (Figs. 1 and 3); since activation is slow, however, I_{ss} does not contribute appreciably to the peak. Rather, I_{ss}, together with $I_{K,slow}$, determines current amplitude at times late after the onset of depolarization(s), whereas $I_{to,f}$ and $I_{to,s}$, which inactivate rapidly ($\tau_{decay} \approx 60$ and 200 ms, respectively) also do not contribute to the late currents. The fact that peak current densities are significantly lower in $I_{to,s}$- than $I_{to,f}$-expressing cells and that $I_{K,slow}$ densities are similar suggests that action potentials likely are broader in $I_{to,s}$-expressing adult mouse ventricular myocytes than in cells lacking $I_{to,s}$ and expressing $I_{to,f}$. The finding that $I_{to,f}$ and $I_{to,s}$ are differentially distributed also suggests that there will be differences in action potential waveforms in cells isolated from different regions of the ventricles. In addition, the marked differences in the rates of inactivation and recovery from inactivation for $I_{to,f}$ and $I_{to,s}$ suggest regional differences in rate-dependent variations in action potential waveforms. Further experiments will be necessary to test these hypotheses directly.

Relationship to Previous Studies

Several previous studies have examined outward K^+ currents in adult mouse ventricular cells, and have been focussed primarily on $I_{to,f}$ (Benndorf et al., 1987; Benndorf and Nilius, 1988; Wang and Duff, 1997). The time- and voltage-dependent properties of $I_{to,f}$ described in these studies are quite similar to those reported here, in that current activation and inactivation are rapid. The results presented here also show that mouse ventricular $I_{to,f}$ recovers from steady state inactivation very rapidly ($\tau = 27$ ms), and the currents resemble those of $I_{to,f}$ in a variety of other species (Campbell et al., 1995; Barry and Nerbonne, 1996; Giles et al., 1996). The slowly inactivating outward K^+ current, $I_{K,slow}$, has also been identified previously in adult mouse ventricular myocytes (London et al., 1998a; Zhou et al., 1998). The mean $I_{K,slow}$ inactivation time constant reported in these studies was 595 ± 29.3 ms ($n = 7$), a value that is considerably smaller than the time constant (mean ≈1,200 ms, $n = 132$) determined here for $I_{K,slow}$. The reason for the discrepancy between the absolute values of these time constants is unclear. Similar to previous findings (London et al., 1998a), however, $I_{K,slow}$ is highly sensitive to 4-AP. A current sensitive to micromolar concentrations of 4-AP and referred to as I_{sus} (for sustained), has also been described by Fiset et al. (1998). Because I_{sus} was measured at the end of 500-ms voltage steps, however, it almost certainly reflects the sum of I_{ss} and $I_{K,slow}$.

In contrast to $I_{to,f}$ and $I_{K,slow}$, neither $I_{to,s}$ nor I_{ss} has been characterized previously in adult mouse ventricular myocytes. Interestingly, however, $I_{to,s}$ is similar to the novel current recently described in ventricular myocytes isolated from adult Kv4.2W362F-expressing transgenic mice, in which $I_{to,f}$ is eliminated (Barry et al.,

Published May 1, 1999

1998). The time constants of inactivation of the novel current and $I_{to,s}$ are similar, and preliminary experiments suggest that the pharmacological properties of the two currents are also similar (H. Xu and J.M. Nerbonne, unpublished observations). Thus, it seems reasonable to suggest that $I_{to,s}$ is the novel current seen in the Kv4.2W362F transgenics and, further, that the functional expression of this conductance pathway is influenced, and perhaps regulated, by $I_{to,f}$ expression. Further experiments will be necessary to test this hypothesis directly.

Molecular Correlates of Mouse Ventricular $I_{to,f}$, $I_{to,s}$, $I_{K,slow}$, and I_{ss}

Several recent studies focused on identifying the molecular correlates of cardiac transient outward K^+ currents have provided considerable evidence supporting the hypothesis (Dixon and McKinnon, 1994) that α subunits of the Kv4 subfamily underlie $I_{to,f}$ (Fiset et al., 1997; Johns et al., 1997; Barry et al., 1998; Xu, H., H. Li, and J.M. Nerbonne, manuscript submitted for publication). In mouse heart, for example, it has been demonstrated that $I_{to,f}$ is selectively eliminated in both ventricular and atrial myocytes isolated from transgenic animals expressing the dominant negative construct, Kv4.2W362F (Barry et al., 1998; Xu, H., H. Li, and J.M. Nerbonne, manuscript submitted for publication). The finding that the novel transient outward current (i.e., $I_{to,s}$) is expressed in all transgenic cells lacking $I_{to,f}$, in contrast, suggests that Kv4 α subunits do not contribute to $I_{to,s}$. The slow kinetics of inactivation and recovery from inactivation of $I_{to,s}$, however, are reminiscent of the properties of another Kv α subunit, Kv1.4 (Tseng-Crank et al., 1990), that generates slowly decaying transient K^+ currents when expressed in heterologous systems (Comer et al., 1994; Petersen and Nerbonne, 1999). In addition, it was reported recently that regional differences in the properties of the transient outward K^+ currents in ferret left ventricular epicardial and endocardial myocytes are correlated with differences in the expression of Kv4.2/Kv4.3 (epicardium, fast I_{to}) and Kv1.4 (endocardium, slow I_{to}) (Brahmajothi et al., 1998). Although these observations make it tempting to speculate that Kv1.4 underlies mouse ventricular $I_{to,s}$, it has recently been reported that targeted deletion of the Kv1.4 gene does not affect the membrane properties of adult mouse ventricular myocytes (London et al., 1998b). In these experiments, however, mouse ventricular myocytes were randomly dispersed and a rather small number of cells was studied. It is certainly possible, therefore, that the small subset of cells expected to be affected by elimination of Kv1.4 (if indeed this subunit underlies $I_{to,s}$) might not have been identified. Additional experiments aimed at examining regional differences in the K^+ currents expressed in the Kv1.4 knockout mice and the molecular correlate(s) of $I_{to,s}$ will certainly be of interest. In addition, two components of steady state inactivation of $I_{to,s}$ were identified in the experiments here. These could reflect two (molecularly) distinct populations of $I_{to,s}$ channels or, alternatively, the complex gating of a single population of $I_{to,s}$ channels. Further experiments focused on resolving this question will be of interest.

A dominant negative strategy was also exploited recently in the generation of transgenic mice expressing a truncated Kv1.1, *Kv1.1N206Tag* (London et al., 1998a). Electrophysiological experiments revealed that the 4-AP–sensitive, slowly decaying outward K^+ current $I_{K,slow}$ was selectively attenuated in ventricular myocytes isolated from *Kv1.1N206Tag*-expressing mice (London et al., 1998a). These observations, together with the sensitivity of $I_{K,slow}$ to 4-AP, suggest that a member of the Kv1 subfamily, likely Kv1.5, underlies $I_{K,slow}$ (London et al., 1998a). Interestingly, the experiments here have revealed the presence of two components of steady state inactivation of $I_{K,slow}$. The finding of two components of steady state inactivation could reflect the fact that there are two (molecularly) distinct populations of K^+ channels contributing to $I_{K,slow}$ or, alternatively, the complex gating of a single population of $I_{K,slow}$ channels. It will be of interest to pursue further studies on ventricular myocytes isolated from *Kv1.1N206Tag*-expressing animals to determine whether one (or both) component of steady state inactivation is reduced by *Kv1.1N206Tag* expression. Further experiments will also be necessary to define the molecular correlate of the slowly activating and noninactivating component of the mouse ventricular K^+ currents, I_{ss}.

The authors thank Drs. Dianne Barry and Elias Bou-Abboud for many helpful discussions during the course of this work. Also, we thank Ms. Janice Delmar and NPS Pharmaceuticals (Salt Lake City, UT) for providing us with *Heteropoda* toxin-3.

This study was supported by the National Heart, Lung and Blood Institute of the National Institutes of Health and the Monsanto/Searle/Washington University Biomedical Agreement.

Original version received 24 December 1998 and accepted version received 2 March 1999.

Published May 1, 1999

references

Antzelevitch, C., S. Sicouri, A. Lukas, V.V. Nesterenko, D.-W. Liu, and J.M. DiDiego. 1995. Regional differences in the electrophysiology of ventricular cells: physiological implications. *In* Cardiac Electrophysiology: From Cell to Bedside. D.P. Zipes and J. Jalife, editors. W. B. Saunders Co., Philadelphia. 228–245.

Anumonwo, J.M.B., L.C. Freeman, W.M. Kwok, and R.S. Kass. 1991. Potassium channels in the heart: electrophysiology and pharmacological regulation. *Cardiovasc. Drug Rev.* 9:299–316.

Barry, D.M., and J.M. Nerbonne. 1996. Myocardial potassium channels: electrophysiological and molecular diversity. *Annu. Rev. Physiol.* 58:363–394.

Barry, D.M., J.S. Trimmer, J.P. Merlie, and J.M. Nerbonne. 1995. Differential expression of voltage-gated K^+ channel subunits in adult rat heart: relationship to functional K^+ channels. *Circ. Res.* 77:361–369.

Barry, D.M., H. Xu, R.B. Schuessler, and J.M. Nerbonne. 1998. Functional knockout of the cardiac transient outward current, long QT syndrome and cardiac remodelling in mice expressing a dominant negative Kv4 α subunit. *Circ. Res.* 83:560–567.

Benndorf, K., F. Markwardt, and B. Nilius. 1987. Two types of transient outward currents in cardiac ventricular cells of mice. *Pflügers Arch.* 409:641–643.

Benndorf, K., and B. Nilius. 1988. Properties of an early outward current in single cells of the mouse ventricle. *Gen. Physiol. Biophys.* 7:449–466.

Boyden, P.A., and C.D. Jeck. 1995. Ion channel function in disease. *Circulation.* 29:312–318.

Brahmajothi, M.V., D.L. Campbell, R.L. Rasmusson, M.J. Morales, J.M. Nerbonne, and H.C. Strauss. 1999. Distinct transient outward potassium current (I_{to}) phenotypes and distribution of fast-inactivating potassium channel alpha subunits in ferret ventricular myocytes. *J. Gen. Physiol.* 113:581–600.

Campbell, D.L., R.L. Rasmusson, M.B. Comer, and H.C. Strauss. 1995. The cardiac calcium-independent transient outward potassium current: kinetics, molecular properties, and role in ventricular repolarization. *In* Cardiac Electrophysiology: From Cell to Bedside. 2nd ed. D.P. Zipes and J. Jalife, editors. W. B. Saunders Co., Philadelphia. 83–96.

Comer, M.B., D.L. Campbell, R.L. Rasmusson, D.R. Lamson, M.J. Morales, Y. Zhang, and H.C. Strauss. 1994. Cloning and characterization of an I_{to}-like potassium channel from ferret ventricle. *Am. J. Physiol.* 267:H1388–H1395.

Deal, K.K., S.K. England, and M.M. Tamkun. 1996. Molecular physiology of cardiac potassium channels. *Physiol. Rev.* 76:49–67.

Dixon, J.E., and D. McKinnon. 1994. Quantitative analysis of mRNA expression in atrial and ventricular muscle of rats. *Circ. Res.* 75:252–260.

Dixon, J.E., W. Shi, H.S. Wang, C. McDonald, H. Yu, R.S. Wymore, I.S. Cohen, and D. McKinnon. 1996. The role of the Kv4.3 potassium channel in ventricular muscle. *Circ. Res.* 79:659–668.

Fiset, C., R.B. Clark, Y. Shimoni, and W.R. Giles. 1997. Shal-type channels contribute to the transient outward K^+ current in rat ventricle. *J. Physiol. (Camb.).* 500:51–64.

Fiset, C., R.B. Clark, T.S. Larsen, and W.R. Giles. 1998. A rapidly activating, sustained current modulates repolarization and excitation–contraction coupling in adult mouse ventricle. *J. Physiol. (Camb.).* 504:557–563.

Folco, E., R. Mathur, Y. Mori, P. Buckett, and G. Koren. 1997. A cellular model for Long QT Syndrome. Trapping of heteromultimeric complexes consisting of truncated Kv1.1 potassium channel polypeptides and native Kv1.4 and Kv1.5 channels in the endoplasmic reticulum. *J. Biol. Chem.* 272:26505–26510.

Gadsby, D. 1995. Effects of β-adrenergic catecholamines on membrane currents in cardiac cells. *In* Cardiac Physiology: A Textbook. M.R. Rosen, M.J. Janse, and A.L. Wit, editors. Futura Publishing Co., Mt. Kisco, NY. 857–876.

Giles, W.R., R.B. Clark, and A.P. Braun. 1996. Ca^{2+}-independent transient outward current in mammalian heart. *In* Molecular Physiology and Pharmacology of Cardiac Ion Channels and Transporters. M. Morad, Y. Kurachi, A. Noma, and M. Hosada, editors. Kluwer Press, Ltd., Amsterdam, Netherlands. 141–168.

Hamill, O.P., A. Marty, E. Neher, B. Sakmann, and F.J. Sigworth. 1981. Improved patch-clamp techniques for high resolution current recordings from cells and membrane patches. *Pflügers Arch.* 391:85–100.

Ho, C.S., R.W. Grange, and R.H. Joho. 1997. Pleiotropic effects of a disrupted K^+ channel gene: reduced body weight, impaired motor skill, and muscle contraction, but no seizures. *Proc. Natl. Acad. Sci. USA.* 94:1533–1538.

Johns, D.C., H.B. Nuss, and E. Marban. 1997. Suppression of neuronal and cardiac transient outward currents by viral gene transfer of dominant negative Kv4.2 constructs. *J. Biol. Chem.* 272: 24109–24112.

Kass, R.S. 1995. Delayed potassium channels in the heart: cellular, molecular, and regulatory properties. *In* Cardiac Electrophysiology: From Cell to Bedside. 2nd ed. D.P. Zipes and J. Jalife, editors. W. B. Saunders Co., Philadelphia. 74–82.

London, B., A. Jeron, J. Zhou, P. Buckett, X. Han, G.F. Mitchell, and G. Koren. 1998a. Long QT and ventricular arrhythmias in transgenic mice expressing the N terminus and first transmembrane segment of a voltage-gated K^+ channel. *Proc. Natl. Acad. Sci. USA.* 95:2926–2931.

London, B., D.W. Wang, J.A. Hill, and P.B. Bennett. 1998b. The transient outward current in targeted mice lacking the potassium channel gene *Kv1.4*. *J. Physiol. (Lond.).* 509:171–182.

Lyons, G.E., S. Schiaffino, D. Sasson, P. Barton, and M. Buckingham. 1990. Developmental regulation of myosin gene expression in mouse cardiac muscle. *J. Cell Biol.* 111:2427–2436.

Näbauer, M., and S. Kääb. 1998. Potassium channel down regulation in heart failure. *Cardiovasc. Res.* 37:324–334.

Näbauer, M., D.J. Beuckelmann, and E. Erdmann. 1993. Characteristics of transient outward current in human ventricular myocytes from patients with terminal heart failure. *Circ. Res.* 73:386–394.

Nerbonne, J. 1998. Regulation of voltage-gated K^+ channel expression in the developing mammalian myocardium. *J. Neurobiol.* 37: 37–59.

Ng, W.A., I.L. Grupp, A. Subramaniam, and J. Robbins. 1991. Cardiac myosin heavy chain mRNA expression and myocardial function in the mouse heart. *Circ. Res.* 68:1742–1750.

Palermo, J., J. Gulick, M. Colbert, J. Fewell, and J. Robbins. 1996. Transgenic remodelling of the contractile apparatus in the mammalian heart. *Circ. Res.* 78:504–509.

Perozo, E., R. MacKinnon, F. Benzanilla, and E. Stefani. 1993. Gating currents from a nonconducting mutant reveal open–closed conformations in *Shaker* K^+ channels. *Neuron.* 11:353–358.

Peterson, K.R., and J.M. Nerbonne. 1999. Expression environment determines K^+ current properties: Kv1 and Kv4 α subunit-induced K^+ currents in mammalian cell lines and cardiac myocytes. *Pflügers Arch.* 437:381–392.

Ribera, A.B. 1996. Homogeneous development of electrical excitability via heterogeneous ion channel expression. *J. Neurosci.* 16: 1123–1130.

Smart, S.L., V. Lopantsev, C.L. Zhang, C.A. Robbins, H. Wang, S.Y. Chiu, P.A. Schwartzkroin, A. Messing, and B.L. Tempel. 1998. Deletion of the Kv1.1 potassium channel causes epilepsy in mice. *Neuron.* 20:809–819.

Published May 1, 1999

Ten Eick, R.E., J.R. Houser, and A.L. Bassett. 1989. Cardiac hypertrophy and altered cellular activity of the myocardium. *In* Physiology and Pathophysiology of the Heart. 2nd ed. N. Sperelakis, editor. Martinus Nijhoff, Boston, MA. 573–594.

Tseng-Crank, J.C.L., G.-N. Tseng, A. Schwartz, and M.A. Tanouye. 1990. Molecular cloning and functional expression of a potassium channel cDNA isolated from a rat cardiac library. *FEBS Lett.* 268:63–68.

VanWagoner, D.R., A.L. Pond, P.M. McCarthy, J.S. Trimmer, and J.M. Nerbonne. 1997. Outward K^+ current densities and Kv1.5 expression are reduced in chronic human atrial fibrillation. *Circ. Res.* 80:772–781.

Wang, L., and H.J. Duff. 1997. Developmental changes in transient outward current in mouse ventricle. *Circ. Res.* 81:120–127.

Wilde, A.A.M., and M.W. Veldkamp. 1997. Ion channels, the QT interval and arrhythmias. *Pace (Pacing Clin. Electrophysiol.).* 20:2048–2051.

Xu, H., J.E. Dixon, D.M. Barry, J.S. Trimmer, J.P. Merlie, D. McKinnon, and J.M. Nerbonne. 1996. Developmental analysis reveals mismatches in the expression of K^+ channel α subunits and voltage-gated K^+ channel currents in rat ventricular myocytes. *J. Gen. Physiol.* 108:405–419.

Zhou, J., A. Jeron, B. London, X. Han, and G. Koren. 1998. Characterization of a slowly inactivating outward current in adult mouse ventricular myocytes. *Circ. Res.* 83:806–814.